Title: Nano-object release during machining of polymer-based nanocomposites depends on process factors and the type of nanofiller

Authors: Ding Y, Wohlleben W, Boland M, Vilsmeier K, Riediker M

Journal: Annals of Work Exposures and Health

Year: 2017 Nov 10

Issue: 61

Volume: 9

Pages: 1132-1144

DOI: 10.1093/annweh/wxx081

Nano-object Release during Machining of Polymer-based Nanocomposites Depends on Process Factors and the Type of Nanofiller

Yaobo Ding[1,2,3], Wendel Wohlleben[4]*, Mael Boland[4,5], Klaus Vilsmeier[4], Michael Riediker[1,6,7]*

[1] Institute for Work and Health (IST), University of Lausanne and Geneva, Lausanne, Switzerland
[2] Institute of Lung Biology and Disease (iLBD), Helmholtz Zentrum Muenchen, Neuherberg, Germany
[3] Comprehensive Pneumology Center - Member of the German Center for Lung Research (DZL), Munich, Germany
[4] Dept. Material Physics, BASF SE, Advanced Materials Research, Ludwigshafen, Germany
[5] CNRS-Chimie ParisTech, Université Paris 6, Paris, France
[6] IOM Singapore, Singapore
[7] School of Materials Science & Engineering, Nanyang Technological University, Singapore

*Corresponding author: Wendel.Wohlleben@basf.com
*Corresponding author: Michael.Riediker@alumni.ethz.ch

ABSTRACT

We tested the nanomaterial release from composites during two different mechanical treatment processes, automated drilling and manual sawing. Polyurethane (PU) polymer discs (1 cm thickness and 11 cm diameter) were created using different nanomaterial fillers: multiwall carbon nanotubes (MWCNT), carbon black (CB), silicon dioxide (SiO_2), and an unfilled PU control. Drilling generated far more submicron range particles than sawing. In the drilling experiments, none of the tested nanofillers showed a significant influence on particle number concentrations or sizes, except for the PU/MWCNT samples, from which larger particles were released than from control samples. Higher drilling speed and larger drill bit size were associated with higher particle counts. Differences between composites were observed during sawing: PU/CB released higher number concentrations of micro-sized particles compared to reference samples. When sawing PU/SiO_2 more nanoparticle agglomerates were observed. Furthermore, polymer fumes were released during sawing experiments, which was attributed to the process heat. For both drilling and sawing, the majority of the aerosolized particles were polymer matrix materials containing nanofillers (or protruding from their surface), as evidenced by electron microscopic analysis. Results suggest that: 1. processes associated with higher energy inputs are more likely to result in higher

particle release in terms of number concentration; 2. nanofillers may alter release processes; and 3. other types of released particles, in particular polymer fumes from high-temperature processes, must also be considered in occupational exposure and risk assessments.

KEYWORDS: nanoparticle release, composite processing, drilling, sawing, workplace exposure

1. INTRODUCTION

Engineered nanomaterial (ENM) fillers, such as carbon nanotubes (CNTs), carbon nanofibers, carbon black (CB), silicon dioxide (SiO_2), titanium dioxide (TiO_2), or nanoclay, have all been added to different polymer matrices to manufacture nanocomposites with improved material properties (Jog 2006; Hanemann and Szabó 2010; Szeluga, Kumanek, and Trzebicka 2015). During research and development, as well as during the industrial processing of such materials, filler particles can be released, leading to subsequent human exposure (Kuhlbusch et al. 2011; Brouwer 2010). When inhaled, ENMs may cause unwanted toxic effects on humans. In rats, multiwall carbon nanotubes (MWCNTs) were shown to have pathogenic effects similar to those of asbestos (Poland et al. 2008). SiO_2 nanoparticles were found to cause cytotoxicity in human bronchoalveolar cells (Lin et al. 2006). In mice, lung exposure to CB nanoparticles led to a considerable increase in DNA single-strand breakages (Chuang et al. 2015). To date, nanomaterials are still associated with considerable uncertainties related to their hazard and exposure potential (Hunt et al. 2013). Understanding release and characterizing the released particles will help address important knowledge gaps.

In a recent review of nanomaterial release processes, we identified machining of nano-enabled materials among the types of activities that are most importantly contributing to release and subsequent worker exposure (Ding et al. 2017). Particle release from nanocomposites was proposed to be affected by various process parameters and material properties, such as the type of treatment, environmental conditions (e.g., temperature, humidity), matrix properties (e.g., brittleness, degradation potential), and filler type, physical form (e.g., fiber length, orientation), content, and dispersion (Harper et al. 2015; Kingston et al. 2014;

Schlagenhauf, Nüesch, and Wang 2014). Comparing different processes and associated release patterns is especially interesting from an occupational hygiene viewpoint. Previous investigations have determined levels of nanoparticle release during different mechanical and chemical processes. Dry machining of polymer-alumina-CNT composites in a laboratory simulation study led to considerable release of nano-sized and fine particles and fibers (Bello, Wardle, Yamamoto, Guzman deVilloria, et al. 2009; Bello et al. 2010). In a study where an electric table saw was used to cut carbon nanofiber composites, above 10,000 particles per cm^3 (diameter about 400 nm or larger) were measured close to the emission source. (Mazzuckelli et al. 2007; Methner, Crawford, and Geraci 2012). A greater release of nanoparticles was also recorded from the friction of mechanical shocks and abrasion processes on composite surfaces (Golanski et al. 2012). By studying the mechanical properties and crushing behavior of composites, Sachse et al. demonstrated that nano-sized particles were emitted from polymer composites reinforced with nano- and microsilica, as well as with nanoclay fillers. However, other studies found no significant release from nanocomposites, in comparison to the control materials, and in certain cases the generation of airborne particles was even lower. During the thermal cutting of polystyrene (PS) foam, over 99% of the filler particles were found to be embedded in submicron aerosol particles (Zhang et al. 2012). An investigation of nanoclay polymer composites during drilling showed that integrating nanofillers into the base polymer decreased particle concentrations (Sachse, Silva, Zhu, et al. 2012). During the sanding of thermoplastic polyurethane (PU)/CNT composites, no free nanofillers were observed, and it was concluded that more than 97 wt% of the filler materials were still embedded in the polymer matrix (Wohlleben et al. 2013). However, despite the efforts made so far, conclusive predictions about particle release, whether from specific nanocomposites or specific processes, remain difficult to make.

In this study, we drilled and sawed cross-linked PU-based composites reinforced with three different types of nanofillers at 0.09% content, which is in the range of filler concentrations commonly used in commercial products: for example, CNT composites start to show electrical conductivity with a filler content as low as 0.002% (Bauhofer and Kovacs 2009), and also for other fillers such as carbon black,

concentrations below 2% are added in composites when the role of the filler is to improve the UV-stability against degradation for use in outdoor environments (Buxbaum and Pfaff 2006). Drilling is a process associated with high-speed mechanical shear forces to produce a hole; sawing is considered a relatively low-speed process with a limited contact area with the material (Canady et al. 2013). To the best of our knowledge, there have been few investigations comparing particle release scenarios in these two processes. PU is a matrix material rarely studied in release tests. In the present study, release tests for these two processes were set up, validated, and used to examine how process parameters influenced the particle number concentration, size range, and particle morphology of the aerosols released.

2. MATERIALS AND METHODS

2.1 Materials

The materials tested were polymer composites reinforced using different organic or inorganic nanomaterial fillers. The base polymer was partially cross-linked PU synthesized using a prepolymer process handled by our project partner, Nanocyl. Three types of nanocomposites containing 0.09% (w/w) filler materials of fumed silica (SiO_2, ABCR, primary size: ca. 20 nm), MWCNTs (NC7000, Nanocyl, average diameter/length: 9.5 nm/1.5 μm, BET surface area: 250-300 m^2/g) and CB (Vulcan XC72, Cabot, primary size: 30-60 nm, specific surface area: 250 m^2/g) were tested. This low filler content is of commercial relevance, as we measured a reduction of the PU electrical resistivity by nearly 6 orders of magnitude to 6.0 x 10^5 Ω/cm for the PU/CNT, confirming percolation. Conductivity is not achieved by PU/CB at this concentration, confirming the potential technical advantage of CNT as filler to achieve antistatic / conductive polymer.

The Pure PU samples were used as negative controls. The visual appearance of the samples, as well as the transmission electron microscope (TEM) characterizations of the morphologies and the distribution of the filler particles in the matrix, is shown in **Figure 1**.

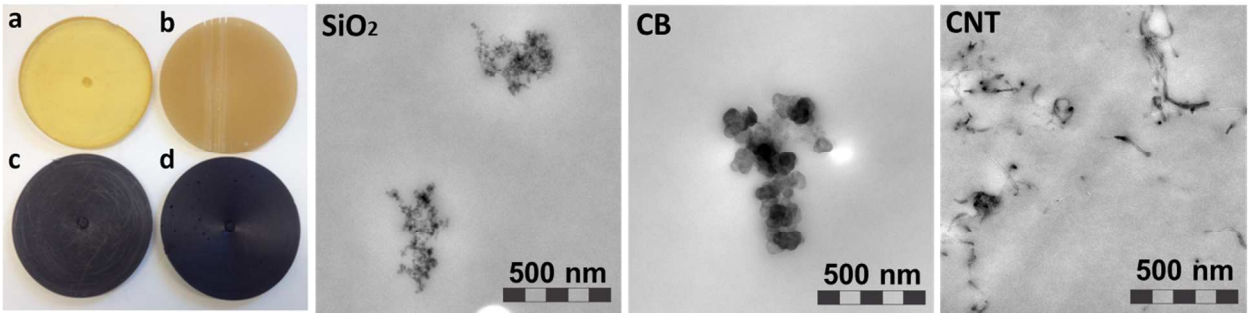

Figure 1. Photo of tested samples (a - PU; b - PU/SiO_2; c - PU/CB; d - PU/MWCNT) and TEM images of a cross-section of the samples with the three filler types. Sample dimensions: 11 cm Φ x 1.0 cm thickness, disc.

2.2 Test Setups

2.2.1 Automatically Controlled Drilling System

Drilling tests were done inside a transparent plastic chamber (154 L volume, **Figure 2**, left) in order to separate the drilling process from the outside atmosphere. The sample was fixed to a rotatable round plate that allowed the drilling position to be changed between drilling tests. Only the drill bit was inside the chamber. The pressure of the bit on the composite material was controlled by a spring pulling the sample towards the drill bit (drill force: 17 N). An infrared thermometer with an effective sensing zone of 1 cm^2 was used to continuously monitor temperature changes during drilling. The sampling ports for particle measurements were pointed towards the drill hole. A DISCmini (Matter Aerosol, Switzerland) was used for measuring particle number concentration and mean diameter in the 10–300 nm size range. In addition, gold filters (0.2 um pore size, Φ25 mm, APC) were used to collect airborne particles for subsequent analysis using a scanning electron microscope (SEM). The sampling flow rate was 5 L/min. Filtered air was used to flush the chamber before each test until the background particle concentration was below 200 #/cm^3 (DISCmini, 1 L/min flow rate). Five drilling tests were conducted, one after the other, for each sample type. In order to clean out the residual particles from the previous drilling tests, the chamber was flushed using a 30 L/min air flow for at least 15 min. Each drilling test lasted about 1 min. Different drilling speeds and drill bit sizes were used (**Table 1**).

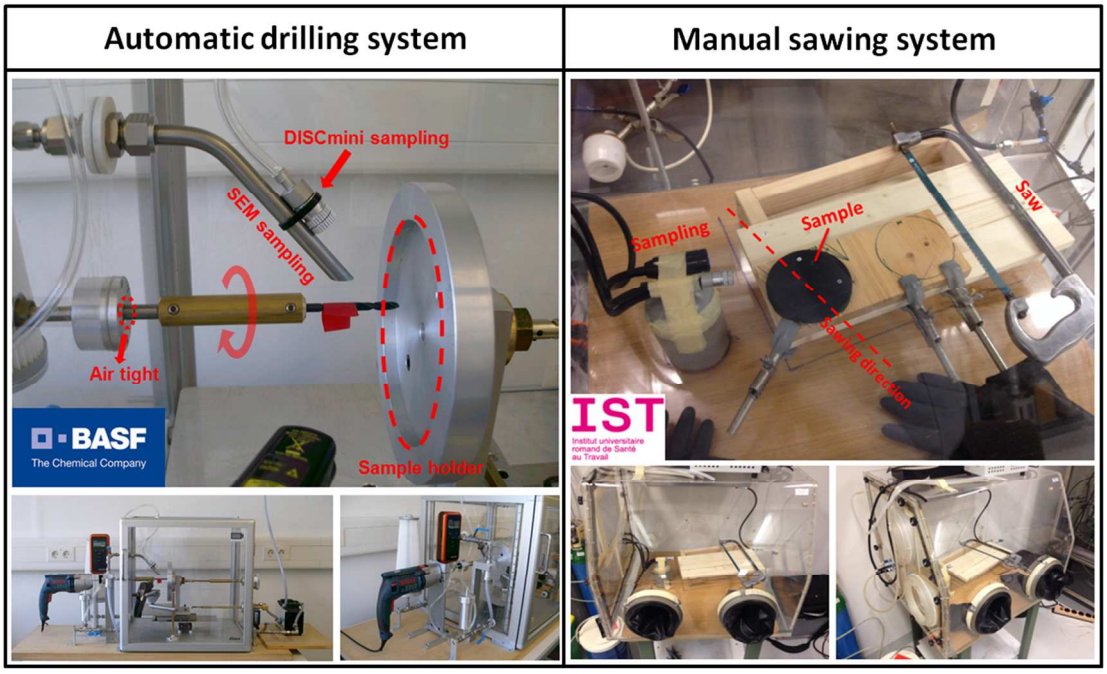

Figure 2 Photos of the drilling (left) and sawing (right) setups used in the tests

Table 1. Drilling test parameters.

		Drilling speed, rpm		
		1200 (S3)	1550 (S5)	1880 (S7)
Drill bit size, mm	4	-	All	SiO_2
	8	MWCNT	MWCNT	All

*Entire range of drilling speeds: 900–2,900 rpm from settings (S) 1-10.

2.2.2 Manual Sawing System

A laboratory glove box (284.9 L volume) was used to enclose the sawing experiment (**Figure 2**, right). Samples were tightly fixed to a wooden support. The saw was operated via the box's rubber gloves. The enclosure was flushed with high flow rates of filtered air (50 L/min) until the background particle concentration was below 20 #/L. Sampling ports were placed about 10 cm from the cutting position to the side of the main sawing axis. Sampling was done using a DISCmini (1 L/min inflow), a filter sample holder (2 L/min inflow) equipped with a gold-coated track-etched filter (0.8 µm pore size), a sample collector for transmission electron microscopy (Ecomesure; TEM grid - copper grid coated with Formvar

carbon film; sample flow rate: 0.3 L/min), and an optical particle counter (OPC, 1 L/min inflow, GRIMM, model 1.109). The OPC measures particle number and size distributions from 250 nm to 32 μm. A thermometer (Celsimeter®, K-thermocouple: -50°C ~ +1000°C, Spirig, Switzerland) was used for measuring the temperature of the manual saw's blade (blade dimension: 300×12.5 mm, HSS-high speed steel, technocraft®). Four to five cuts were conducted in each test. Sawing began in the center of the sample, and the distance between sawing positions during the test was about 2 mm. The length of the cut was thus kept approximately the same. The material was not completely sawn through in order to avoid touching the wooden support. Each sawing session lasted about 5–7 min. During this period, the air supply to the enclosure was set at 6 L/min to replace the air drawn for sampling needs (total flow drawn by sampling instruments ≈ 4.3 L/min). After each cut, sampling continued for 10 min. Between cuts, the chamber was flushed at a flow rate of 50 L/min filtered air for about 15–20 min to clean out residual particles.

2.3 Data Analysis

To estimate the number of particles released per drilling event, we first averaged the peak particle concentrations generated after each drilling test. The peak concentration was determined from the fitted curve of moving averages over 50 seconds (Figure S1). The total particle release from a single drilling event was then estimated by assuming that: a) the chamber was a well-mixed environment in which homogeneous particle concentrations were present at the end of a drilling event; and b) that all released particles in the size range analyzed by the DISCmini were still airborne during this peak period of the drilling event. The particle loss to the instrument's sampling flow during the drilling event (ca. 1 min) was not taken into account since the sampling flow rate was relatively low. The total number of released particles counted was thus determined by integrating the peak concentration (averaged from the period when particle concentration became stable shortly after drilling stopped) over the chamber volume. The total number of background particles was determined based on average background concentration during the 15–30 min before each test. The net release was then calculated by subtracting background particles

from the total number of released particles. The analysis of variance (ANOVA) of the average number and mean size of the particles from different samples was performed using Stata software (Stata CorpLP, Texas, USA). P-values <0.05 were considered statistically significant.

3. RESULTS

3.1 Release Scenarios in the Drilling Tests

3.1.1 Influences of Types of Nanofiller and Drilling Parameters

The net particle release (corrected for background particles) and particle sizes under the various test conditions are shown in **Figure 3**. The particle number concentration and mean size obtained from replicate tests for the different materials were repeatable with standard deviations of <8% (number) and <15% (diameter), as shown in **Table 2**. The PU/CNT sample released the lowest number of particles compared to the other samples, with both the small and big drill bits and at different drilling speeds (**Figure 3** a,b). In general, the number of particles released increased with the larger drill bit size and the faster drilling speed. However, the relative order between the different types of nanomaterial filler remained unchanged. The SiO_2- and CB-reinforced composites released similar numbers of particles to the blank sample. The total number of particles generated by drilling a single hole through the sample ranged from 4.3×10^7 to 2.2×10^9 particles using the two sets of experimental conditions. The mean diameter of the released PU/CNT particles was around 100 nm and above 200 nm for the two sets of conditions, which was the largest from among the samples (**Figure 3**e,f). Particle release increased with higher drilling speeds (**Figure 3**c). Particle generation soared from 4.3×10^7 to 65.2×10^7 particles (about 15.2 times higher) when using the bigger drill bit (**Figure 3**d). The variations in results were larger (shown by the error bars) when using high drilling speeds or the big drill bit. Higher drilling speed resulted in a slightly lower average particle sizes (**Figure 3**g), while larger drill bit increased particle diameter (**Figure 3**h). During the experiment, the local temperature on the drilling sites remained below

70°C (Figure S4), and thus below the temperature at which the polymer matrix or thermal degradation products can evaporate and recondense into aerosol particles.

Replicate Test	PU		PU/CNT		PU/SiO_2		PU/CB	
	N, #/cm^3	D, nm	N, #/cm^3	D, nm	N, #/cm^3	D, nm	N, #/cm^3	D, nm
Background	262	-	288	-	186	-	141	-
Drill 1	743	63.7	626	101.5	649	85.3	581	59.7
Drill 2	648	54.1	540	97.7	732	65.6	610	53.1
Drill 3	651	51.1	577	89.7	651	60.9	573	53.8
Drill 4	640	71.0	501	94.7	656	60.8	558	55.1
Drill 5	695	52.0	585	100.5	-	-	693	58.8
Mean	675	58.4	566	96.8	680	68.1	603	56.1
S.D.	38.8	7.7	42.2	4.3	37.4	10.1	48.0	2.7
S.D., %	5.74%	13.27%	7.46%	4.42%	5.50%	14.78%	7.95%	4.78%

Table 2. Particle number concentration, N (#/cm^3), and geometric mean diameter, D (nm), for replicate tests (Φ/drill, 4 mm; drill speed setting, S5). All measurements recorded with a DISCmini (size range 10–300 nm). The differences in particle number were statistically significant for PU-PU/CNT pair (P=0.0052) and for PU-PU/CB pair (P=0.0473), but not for PU-PU/SiO_2 pair (P=0.9075). The difference in size was only significant for PU-PU/CNT pair (P=0.0001), but not for PU-PU/SiO_2 pair (P=0.1905) and PU-PU/CB pair (P=0.6103).

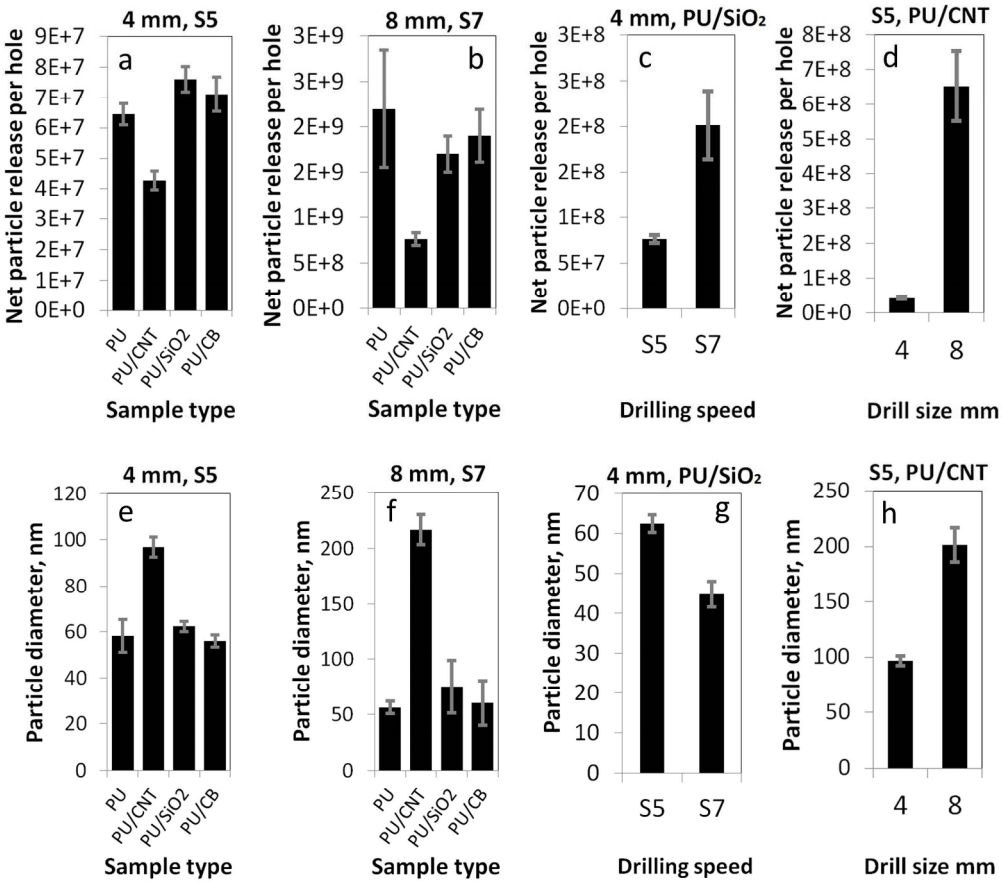

Figure 3. Influence of types of nanomaterial filler, drill speed setting (S5 or S7), and bit diameter (4 mm or 8 mm) on the net release of particles and their mean diameter (size range: 10–300 nm). The statistical analysis: a) $p=0.0056$ (group), $p=0.013$ (PU-PU/CNT pair), $p>0.1$ (other pairs); b) $p=0.004$ (group), $p=0.0205$ (PU-PU/CNT pair), $p>0.1$ (other pairs); c) $p=0.006$; d) $p<0.001$; d) $p=0.006$; d) $p<0.001$;e) $p<0.001$ (group), $p<0.001$ (PU-PU/CNT pair), $p>0.1$ (other pairs); f) $p<0.001$ (group), $p<0.001$ (PU-PU/CNT pair), $p>0.1$ (other pairs). g) $p<0.001$; h) $p<0.001$.

3.1.2 Morphological Analysis

Released airborne particles were collected and analyzed by SEM, as shown in **Figure 4**. All the particles collected had the visual appearance of polymer matrix materials. The diameters of pieces of drilled-out material were usually in the order of a few micrometers. Different geometries were observed for the various composite types, such as irregular thin flakes for the PU/CNT samples or lumps of materials for

the other samples. **Figure 4** (e–h) shows close-up images of the surface morphologies of the three filler samples. Numerous bright spots appeared on the PU/CNT and PU/CB composites; their size and apparent higher electron density can be attributed to protrusions of nanofiller on the particle surface. For PU/CNT samples, elongated features were clearly visible at the surface (**Figure 4**g); these matched the known diameter and length of the specific CNTs used. In contrast, a cluster of hollow structures was observed on the PU/SiO_2 sample (**Figure 4**h). Most of the released particles were matrix materials with protrusions of nanofiller particles at the surface. The particle coverage on the surface of the aerosol filters remained relatively sparse, resulting in a considerable statistical uncertainty from the microscope observations. Thus, although no individual primary nanoparticles were observed during the drilling experiments, their occurrence cannot be completely excluded.

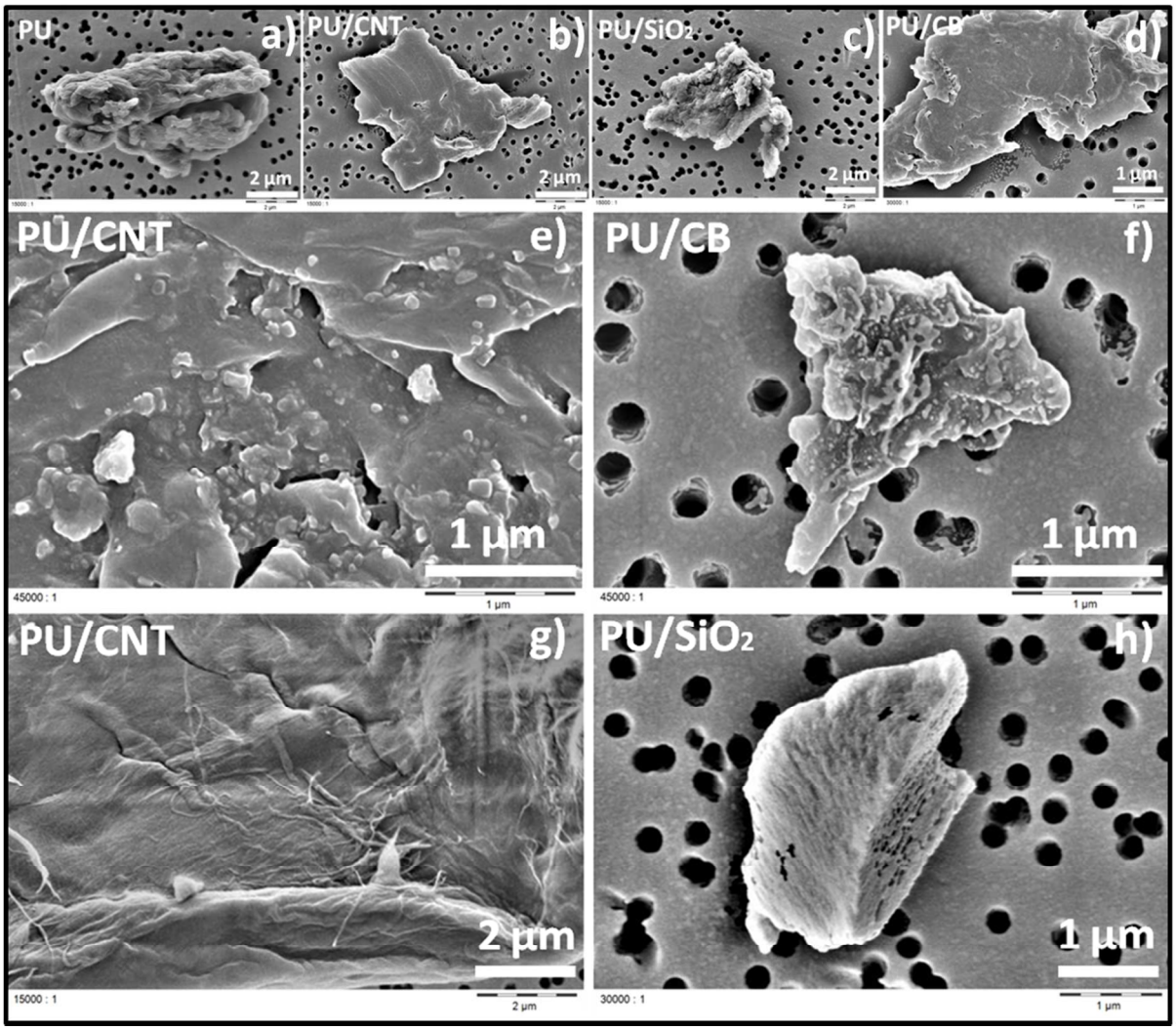

Figure 4. Surface morphologies of particles released in the drilling tests.

3.2 Release Scenarios in the Sawing Tests

3.2.1 Influence of Types of Nanofiller

Original particle number concentrations measured by the two devices are summarized in **Table 3**. Compared to drilling, sawing resulted in clearly different particle concentrations, in different size ranges, for the various tested nanofiller composites. In the size range of 10-300 nm, the measured concentrations by DISCmini (54-167 #/cm^3) were less than the manufacturer established lower detection limit of the device (1,000 #/cm^3). Thus, the difference in particle release level in this size range among the four

composite types cannot be firmly established on the basis of the machine readouts. In comparison, in the 0.25–32 μm size range, the release level for the PU/CB sample was considerably higher than for the other three materials (**Figure 5**). The PU/CNT registered minor increases over control materials, and the PU/SiO_2 samples remained nearly the same.

	OPC (250 nm – 32 μm), #/cm^3				DISCmini (10–300 nm), #/cm^3			
	PU	PU/CNT	PU/SiO_2	PU/CB	PU	PU/CNT	PU/SiO_2	PU/CB
Backgr.	0.001	0.001	0.021	0.020	40	36	89	30
Cut 1	0.404	1.714	0.519	6.025	36	66	63	57
Cut 2	0.284	1.349	0.489	5.580	30	63	66	46
Cut 3	0.409	1.069	0.594	5.290	1	50	118	44
Cut 4	0.259	1.279	0.384	4.715	-12	50	66	42
Cut 5	0.319	1.074	-	-	14	101	-	-
Mean	**0.335**	**1.297**	**0.497**	**5.403**	**13.75**	**57.25**	**78.25**	**47.25**
S.D.	0.069	0.264	0.087	0.549	19.9	20.9	26.5	6.7
S.D., %	20.6%	20.4%	17.5%	10.2%	144%	36.5%	33.9%	14.2%

Table 3. Summary of particle number concentration results for different samples during the sawing process (results for cut 1 to 5 are background corrected. Note: The default unit of the OPC readings is #/L and it is converted into #/cm^3 in the table for comparison purposes). The difference in OPC mean particle concentrations for the four sample types was significant ($p<0.001$); pairwise differences were all significant ($p<0.05$). DISCmini measurements were below the detection limit of 1000 #/cm^3 established by the manufacturer. The difference in DISCmini machine readouts of the mean particle concentrations for the four sample types was significant ($p=0.0013$); pairwise differences were all significant: PU-PU/MWCNT ($p=0.004$), PU-PU/SiO2 ($p=0.004$) and PU-PU/CB ($p=0.015$).

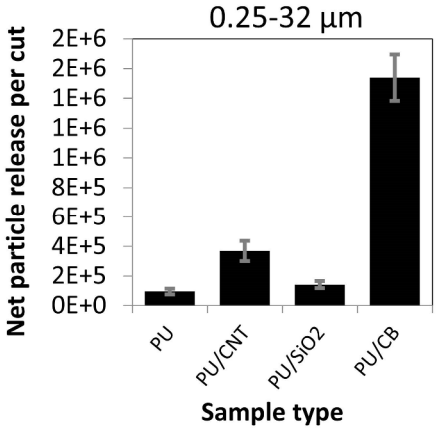

Figure 5. Influence of type of filler on particle release (net release after background correction) in the size range 0.25–32 µm (data from OPC).

3.2.2 Morphological Analysis

The collected airborne samples were analyzed using TEM and SEM (**Figure 6** shows the example of SiO_2 containing composite). Large particles of a few microns in diameter (**Figure 6** a,b) and submicron particles (**Figure 6**c) were found. Small spherical particles around 100 nm or below were also present on the grid (**Figure 6** a–d). In the SEM characterizations, the particle morphologies were often seen as irregular, thick lumps, ranging from 1–10 µm. The surfaces of PU/CB samples appeared to be different from those of other samples, showing scattered bright spots as was also observed for that material in the drilling tests (**Figure 4**). Individual nanofiller particles were not found in the SEM investigations. The particles collected seemed to be materials sawn from the polymer matrix, with a visible nanofiller texture on the surface of certain samples. An analysis of the chemical composition of the PU/SiO_2 sample surface (**Figure 6**i) identified nanofiller content. In addition, a large particle exhibiting a powdered surface and seeming to consist of smaller particles, also appeared on the filter (**Figure 6**j). Chemical analysis confirmed the presence of silicon in this particle.

Particle diameters in the order of 100 nm would be indicative of polymer fumes. This phenomenon is known from an aerosol monitoring study on injection molding sites, where polymer extrusion temperatures reach 200°C and above (Tsai et al. 2008). In our tests, each sawing session typically lasted 5–7 min, which was much longer than the drilling process (~50 seconds). The blade may heat up due to the repeated sawing action, up to a point where the matrix starts to degrade and generate polymer fumes. To test this hypothesis, the blade's temperature was monitored during sawing (Figure S5). The thermocouple sensor was fixed to the blade using a metallic tape in order to detect temperature changes during sawing sessions. The temperature started to rise as soon as sawing began, and it rapidly (within approximately 1.5 min) reached a stable value of about 120°C. The test's nanocomposite samples were

synthesized between 80°C and 100 °C, thus it is likely that matrix materials at the sawing line were degraded by the blade's heat and subsequently released polymer fume particles.

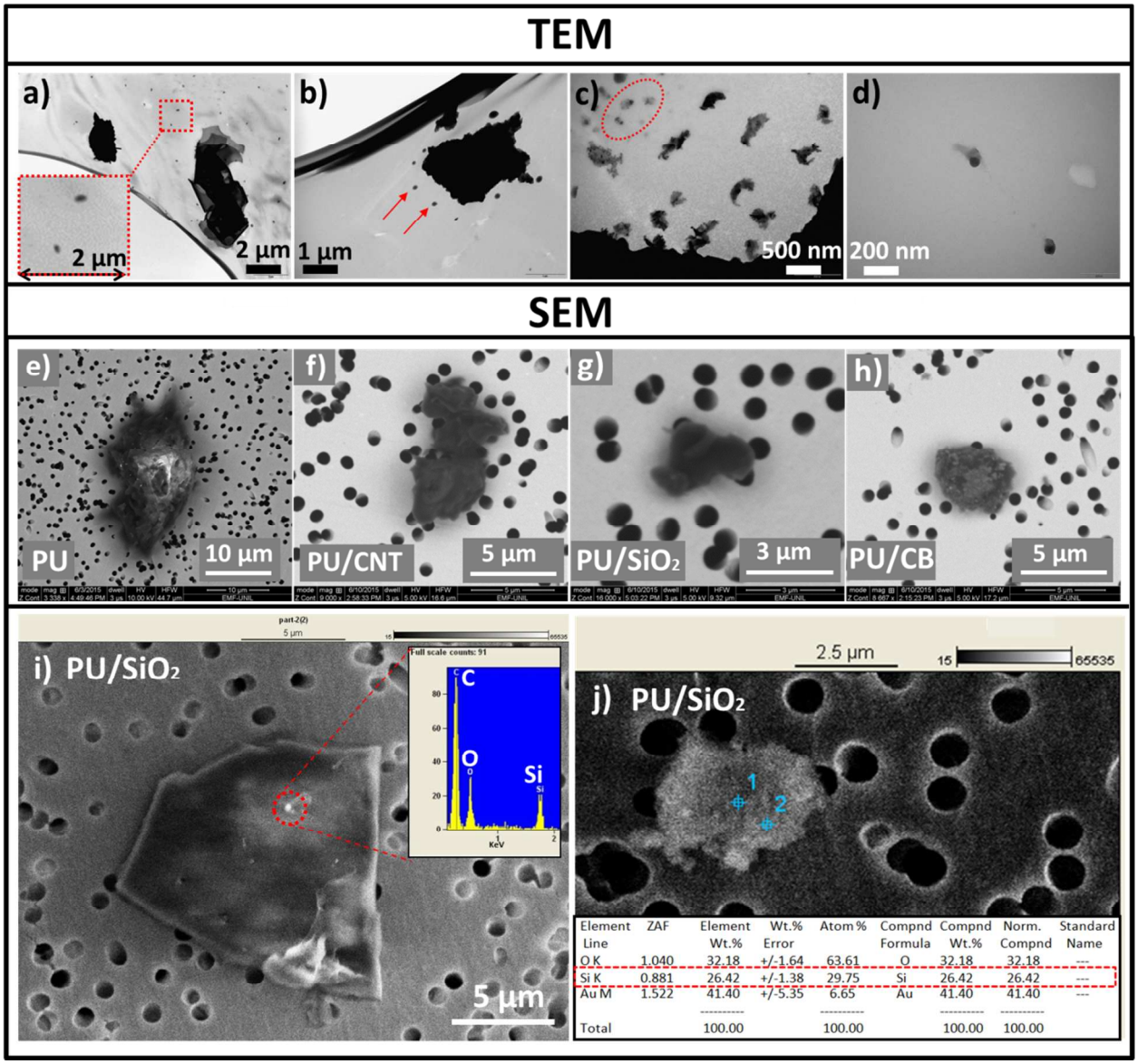

Figure 6. TEM and SEM observations of released particles from the sawing tests: a–d, PU.

4. DISCUSSION

4.1 Effects of Nanofillers

We observed that nanofiller particles and fibers were present on the surface of released matrix materials; this corresponds with earlier reports (Ogura et al. 2013; Cena and Peters 2011; Fleury et al. 2013; A. Hellmann 2012; Devaprakasam et al. 2008; Schlagenhauf et al. 2012). The protrusion of CNTs was attributed to their greater tensile strength; they were pulled out of the fracture interface as the matrix is ripped into particles (Huang et al. 2012). However, Wohlleben et al. did not observe protruding CNTs from sanding fragments; they attributed this to the reflow behavior of the soft thermoplastic polyurethane matrix (600% elongation at break) around the filler particles during destruction (Wohlleben et al. 2013). In our tests, the stronger, partially cross-linked PU matrix was expected to limit flow processes, which explains why the nanofillers were exposed on the particle surfaces. The hollow structures shown on the surface of PU/SiO_2 (**Figure 4**) seemed to be cavities left behind by detached SiO_2 nanofillers. The cavity sizes (100–200 nm) corresponded roughly to the size of the agglomerates observed in the TEM characterization of the raw sample cross-sections (**Figure 1**). The white spots present on PU/CB (**Figure 4** and **Figure 6**) particle surfaces were likely to be individual or agglomerated filler particles, and this was also suggested by the higher electron density in comparison to the surrounding material.

The very low release level of filler particles in our tests may be due to the low nanofiller content in the composites tested (0.09% w/w). Free CNTs were observed when epoxy composites loaded with 4 wt% CNTs were sanded, but they were not when samples with lower loadings were sanded; this was attributed to incomplete dispersion (Huang et al. 2012). The epoxy-alumina-CNT composites in the dry drilling tests contained 1.3%–2.2% of nanofillers, and airborne clusters of CNTs were released during the treatment (Bello et al. 2010). The dispersion and agglomeration levels of the nanofiller particles in the matrix also influence the possibility that they will detach during mechanical processes. Poor distribution of fillers in composites, as well as their agglomeration, can act as failure points during the destruction process. Clearly different release scenarios were observed between samples with poor filler dispersion and those showing good distribution (Golanski et al. 2012). The identification of large SiO_2 filler particles after the sawing tests in our study may be in part due to its strong agglomeration state thus loose

connection to the matrix. The distinct release scenarios from the three types of nanocomposite may be attributable to nanofillers' properties. The interlocking and reinforcement effects of MWCNTs can reduce particle generation and increase particle size. The tensile modulus of the carbon nanotubes is much larger than that of a PU matrix. Their long, tube-like geometries may help connect different parts of the composite and prevent large-scale destruction. The same effect has been observed in the dry machining of nanocomposites: fewer airborne particles were generated from a CNT-alumina composite than from the base alumina composite alone (Bello, Wardle, Yamamoto, deVilloria, et al. 2009; Bello et al. 2010). Furthermore, PU/CNT composites generated larger fragments than the control matrix (Wohlleben et al. 2013). A similar strengthening effect was also seen during drilling activities after nanoclay fillers were added to a PA6 matrix (Sachse, Silva, Zhu, et al. 2012). The higher particle generation from drilling and sawing PU/CB composites may be caused by increased brittleness of the matrix. There is evidence of embrittlement when carbon black was added to polymer matrices (Rudolph D and Kalidas R 1976; R. Satheesh Raja ; Kaynak, Polat, and Yilmazer 1996). This effect on particle release is similar to that caused by different types of matrix (e.g., harder vs. softer matrices), and this is discussed in the following sections.

4.2 Effects of Process Characteristics

The treatment types (drilling and sawing) and test conditions (e.g., tool geometry and speed) also influenced the number and size of the particles released. Highly dynamic processes such as sanding, drilling, and grinding are more efficient at destroying solid materials than less dynamic processes including abrasion, sawing/scratching, and mechanical shock. Furthermore, processes treating larger surface areas on samples are likely to detach more materials from the matrix (e.g., sanding). Golanski et al. provided evidence that rotating steel brushes and graving tools were more efficient at removing CNTs from hard polymer coating surfaces than other abrasion processes (Golanski et al. 2012). Also, metallic rakes were effective at detaching nanoparticles from fabric nanomaterials by scratching. In our tests, the greater numbers of particles released using faster rotation speeds and larger drill bits in our tests can be

linked to the higher energy levels existing under those conditions. Similar results have been seen during solid core drilling of epoxy-based composites (Bello et al. 2010).

Treatments featuring a significant generation of heat may thermally decompose the polymer matrix and release nanoscale fume particles. This phenomenon is often observed in studies investigating high-temperature processes. Particle numbers decreased by 99.9% when a 190°C thermodenuder was used, which implies that the nanoscale particles released were likely to have been volatile, high-melting-point contents that evaporated due to the heat friction caused by grinding (Ogura et al. 2013). A visible smoke plume was generated during the dry drilling of epoxy composites (Bello et al. 2010). Volatile organic compounds, peaking at 70 nm diameter, were released during the thermal cutting of PS and its derivatives (Zhang et al. 2012). For the identical PU and PU/CNT materials as in the present study, thermal decomposition at temperatures ramping from 20°C up to 800°C were investigated. By detailed analysis of the emitted aerosols (gas phase CO analysis, particulate analysis by NMR, FTIR, SMPS, optional thermodenuder), it was found that the aerosol release is dominated by volatile organic compounds with diameters ranging from 20 nm to 200 nm (Sotiriou et al. 2015). In contrast to the ash, the aerosol was not significantly affected by the presence of the CNTs (Sotiriou et al. 2016). This is consistent with present observations and lends further support to our interpretation of process-related VOC emissions by drilling and sawing.

We can compare further to weathering as a process that induces chemical degradation of the matrix, in synergy with weak or intermediate mechanical stresses. The identical set of materials (PU with SiO_2, CB or CNT) was studies in detail for its releases by simulated weathering, and the released fragment morphologies are very different from the sanding or drilling released fragments. Thus, the process is decisive to determine release properties. However, also in that case it was found that the nanofillers modulate the release rates, specifically a reduction by CNT, and an increase by SiO_2 (Wohlleben et al. 2016).

4.3 Matrix Effects

Studies investigating mechanical processes have commonly revealed irregular shapes and significant surface roughness on matrix particles (Van Landuyt et al. 2012; Wohlleben et al. 2013; Wohlleben et al. 2011; Sachse, Silva, Irfan, et al. 2012; Ogura et al. 2013). This was attributed to the ductile nature of polymers that stems from the viscoelastic nature of polymer materials and their special molecular arrangement (Van Krevelen and Te Nijenhuis 2009). The deformation occurring under external loads results in the molecular chains rearranging themselves into new positions and structures (Jansen 2008). As a consequence, there is a tendency for surfaces to become rough, producing lumps, flakes, or layers of materials (**Figure 4** and **Figure 6**).

The nature of the composite matrix material seems to play an important role in the release process. In general, harder materials tend to be more brittle, which means they break more easily into small pieces under deformation. There is a propensity for crevices and cracks to form in brittle materials (Berry 1963). The cross-linked PU used in our test is relatively soft (tensile strengh: 37 MPa, 100% modulus: 12 MPa) compared to the materials used in previously reported studies, such as epoxy (Bello, Wardle, Yamamoto, Guzman deVilloria, et al. 2009; Bello et al. 2010), PA (Sachse, Silva, Zhu, et al. 2012), PVC (Golanski et al. 2012), PS (Ogura et al. 2013; Zhang et al. 2012), and inorganics including bricks (Shandilya, Le Bihan, and Morgeneyer 2014) or cement paste (Wohlleben et al. 2011). The dry drilling of Al_2O_3-epoxy-CNT composites resulted in 3.9×10^6 to 1×10^7 #/cm^3 particle concentrations in the 5.6–560 nm range, using a similar set of drilling speeds (725–1355 rpm) and drill bit diameters (1/4" and 3/8", = 0.64 and 0.95 cm, respectively) to our study (Bello et al. 2010). In comparison, Wohlleben et al. recorded airborne particle numbers below 1000 #/cm^3 during abrasion tests on thermoplastic PU composites (Wohlleben et al. 2013); this is close to the values seen in our tests. The majority of the particles released in these studies were found to be the matrix materials containing nanofillers. The relatively low particle number concentrations obtained in our experiments were in line with the suggestion made by Wohlleben et al. that matrix rigidity has a greater influence on the properties of the released aerosol than the nanofiller

materials do. Softer matrices are less likely to release filler particles and tend to produce larger fragments; this was observed in several other studies (Gohler et al. 2010; Schlagenhauf, Nüesch, and Wang 2014; Harper et al. 2015).

4.4 Limitations

During the sawing experiments, the DISCmini provided machine readouts at concentrations below 1,000 #/cm^3, which is below the lower detection limit proposed by the manufacturer. This makes the interpretation of total net particle releases in this size range difficult. We see clear statistical difference between different test materials. However, the absolute release values in this concentration range should be viewed with caution. Yet, the conclusion that sawing released far less submicron particles (<< 1,000 #/cm^3) than drilling is clearly supported by the OPC results. During initial experiments, an SMPS was operated in parallel to the DISCmini. However, due to the very low and rapidly changing particle concentrations during the course of the sawing operations (5-7 min), the SMPS was not used in the reminder of the experiments.

5. CONCLUSIONS

In this study, we compared scenarios involving the release of nano-objects resulting from two distinct mechanical processes: drilling and sawing. Automatic, machine drilling released greater numbers of particles than manual sawing did. Different drilling parameters modified the intensity of particle release by up to several orders of magnitude. Comparing to pristine samples, PU/CNT composite produced less but larger aerosol particles due to the interlocking effect of the nanotubes. The other types of nanofiller did not substantially influence the results of the release scenarios. Free particles of the filler material were not observed. Instead, the filler particles were visible as protrusions on the surface of cut PU residues. In comparison, the sawing tests generated relatively low particle number concentrations. However, the process produced intense heat and, consequently, polymer fumes. Furthermore, the PU/CB samples produced higher particle number concentrations for micron-sized particles.

Although it was possible to detect free SiO_2-filler particles from the sawing sessions, the majority of the released particles were matrix materials containing the nanofiller. It is conceivable that the amount of filler, as well as how well it is distributed within the matrix, plays an important role in determining the intensity of particle release during such machining. Future studies should further characterize the influences of these two variables. To extrapolate to risk assessment, the literature emerging on the hazards posed by the aerosols released during very similar drilling or sanding setups also indicates that fragments of polymer matrix with protrusions of engineered nanomaterials show no more toxicity than fragments of control polymer without nanofiller (Saber, Koponen, et al. 2012; Saber, Jacobsen, et al. 2012; Wohlleben et al. 2011; Wohlleben et al. 2013; Saber et al. 2016; Schlagenhauf et al. 2015).

The fact that polymer-fume condensates at the nanoscale were identified in our sawing experiments highlights the importance of investigating process-determined release. This is of direct relevance to risk because at elevated temperatures the products of the thermal decomposition of polymers can lead to medical symptoms such as the influenza-like illness known as “polymer fume fever” (Patel, Miller, and Chomchai 2006; Testud, Sabouraud, and Lecoq-Jammes 2010; Townsend, Vernice, and Williams 1989). However, even below thermal release thresholds, energy-intensive processes such as drilling have a greater potential to release particles. The same principle applies to other process parameters in our drilling tests that are associated with higher energy inputs—faster speeds and larger tool geometry—resulting in higher shear rates. This is in agreement with previous findings (Le Bihan 2013). The possibility that nanofiller particle release is process-dependent cannot be ruled out. Compared to the control samples, the PU/SiO_2 samples generated far more particle release in the sawing experiments than in the drilling ones. Therefore, processing conditions do indeed seem to be the most important factor in determining particle release; they should be considered in detail for the laboratory simulation of particle release phenomena. The present study only tested one matrix material, but the literature indicates that the matrix properties themselves are very important determinants of release rates—rates that are eventually modified by the embedded nanomaterials. These modifications are typically less than one order of magnitude and have

been systematically explored in the present contribution, paving the way for a mechanistic understanding of particle release processes.

SUPPORTING INFORMATION

More details on data analysis methods (determination of average peak concentrations), reproducibility analysis, and monitoring of drilling as well as sawing temperature can be found in the supplementary dataset at https://academic.oup.com/annweh.

ACKNOWLEDGEMENTS

The research work was financially supported by the European Research Council under the European Union's Seventh Framework Programme (FP/2007-2013)/ERC Grant Agreement Nr. 263215. We thank Mr. Gregory Plateel and Dr. Nicolas Concha-Lozano for their excellent support in the laboratory and Mr. Antonio Mucciolo for his assistance in SEM/TEM characterizations at the University of Lausanne's Electron Microscopy Facility.

REFERENCES

A. Hellmann KS, S. Ripperger, M. Berges. (2012) Release of ultrafine dusts during the machining of nanocomposites. Gefahrstoffe – Reinhalt. Luft; 72 473-76.

Bauhofer W, Kovacs JZ. (2009) A review and analysis of electrical percolation in carbon nanotube polymer composites. Composites Science and Technology; 69 1486-98.

Bello D, Wardle B, Yamamoto N, Guzman deVilloria R, Garcia E, Hart A, Ahn K, Ellenbecker M, Hallock M. (2009) Exposure to nanoscale particles and fibers during machining of hybrid advanced composites containing carbon nanotubes. Journal of Nanoparticle Research; 11 231-49.

Bello D, Wardle B, Zhang J, Yamamoto N, Santeufemio C, Hallock M, Virji M. (2010) Characterization of exposures to nanoscale particles and fibers during solid core drilling of hybrid CNT advanced composites. Int J Occup Environ Health; 16 434 - 50.

Bello D, Wardle BL, Yamamoto N, deVilloria RG, Garcia EJ, Hart AJ, Ahn K, Ellenbecker MJ, Hallock M. (2009) Exposure to nanoscale particles and fibers during machining of hybrid advanced composites containing carbon nanotubes. Journal of Nanoparticle Research; 11 231-49.

Berry JP. (1963) The morphology of polymer fracture surfaces. Journal of Polymer Science Part C: Polymer Symposia; 3 91-101.

Brouwer D. (2010) Exposure to manufactured nanoparticles in different workplaces. Toxicology; 269 120-27.

Buxbaum G, Pfaff G. (2006) Industrial Inorganic Pigments.: Wiley.

Canady R, Kuhlbusch T, Renker M, Lee E, Tsytsikova L. (2013) NanoRelease Consumer Products Phase 2.5 Report Book NanoRelease Consumer Products Phase 2.5 Report City.

Cena LG, Peters TM. (2011) Characterization and Control of Airborne Particles Emitted During Production of Epoxy/Carbon Nanotube Nanocomposites. J Occup Environ Hyg; 8 86-92.

Chuang H-C, Chen L-C, Lei Y-C, Wu K-Y, Feng P-H, Cheng T-J. (2015) Surface area as a dose metric for carbon black nanoparticles: A study of oxidative stress, DNA single-strand breakage and inflammation in rats. Atmospheric Environment; 106 329-34.

Devaprakasam D, Hatton PV, Möbus G, Inkson BJ. (2008) Effect of microstructure of nano- and micro-particle filled polymer composites on their tribo-mechanical performance. Journal of Physics: Conference Series; 126 012057.

Ding Y, Kuhlbusch TAJ, Van Tongeren M, Jiménez AS, Tuinman I, Chen R, Alvarez IL, Mikolajczyk U, Nickel C, Meyer J*, et al.* (2017) Airborne engineered nanomaterials in the workplace—a review of release and worker exposure during nanomaterial production and handling processes. Journal of Hazardous Materials; 322, Part A 17-28.

Fleury D, Bomfim JAS, Vignes A, Girard C, Metz S, Muñoz F, R'Mili B, Ustache A, Guiot A, Bouillard JX. (2013) Identification of the main exposure scenarios in the production of CNT-polymer nanocomposites by melt-moulding process. Journal of Cleaner Production; 53 22-36.

Gohler D, Stintz M, Vorbau M, Hillemann L. (2010) Characterization of nanoparticle release from surface coatings by the simulation of a sanding process. Ann Occup Hyg; 54 615 - 24.

Golanski L, Guiot A, Pras M, Malarde M, Tardif F. (2012) Release-ability of nano fillers from different nanomaterials (toward the acceptability of nanoproduct). Journal of Nanoparticle Research; 14 1-9.

Hanemann T, Szabó DV. (2010) Polymer-Nanoparticle Composites: From Synthesis to Modern Applications. Materials; 3 3468.

Harper S, Wohlleben W, Doa M, Nowack B, Clancy S, Canady R, Maynard A. (2015) Measuring Nanomaterial Release from Carbon Nanotube Composites: Review of the State of the Science. Journal of Physics: Conference Series; 617 012026.

Huang G, Park J, Cena L, Shelton B, Peters T. (2012) Evaluation of airborne particle emissions from commercial products containing carbon nanotubes. Journal of Nanoparticle Research; 14 1-13.

Hunt G, Lynch I, Cassee F, Handy R, Fernandes T, Berges M, Kuhlbusch T, Dusinska M, Riediker M. (2013) Towards a Consensus View on Understanding Nanomaterials Hazards and Managing Exposure: Knowledge Gaps and Recommendations. Materials; 6 1090.

Jansen JA. (2008) Understanding the consequence of ductile-to-brittle transitions in a plastic materials failure. ANTEC; 742.

Jog JP. (2006) Crystallisation in polymer nanocomposites. Materials Science and Technology; 22 797-806.

Kaynak A, Polat A, Yilmazer U. (1996) Some microwave and mechanical properties of carbon fiber-polypropylene and carbon black-polypropylene composites. Materials Research Bulletin; 31 1195-206.

Kingston C, Zepp R, Andrady A, Boverhof D, Fehir R, Hawkins D, Roberts J, Sayre P, Shelton B, Sultan Y*, et al.* (2014) Release characteristics of selected carbon nanotube polymer composites. Carbon; 68 33-57.

Kuhlbusch T, Asbach C, Fissan H, Gohler D, Stintz M. (2011) Nanoparticle exposure at nanotechnology workplaces: A review. Particle and Fibre Toxicology; 8 22.

Le Bihan O, Shandilya, N. , Gheerardyn, L. , Guillon, O. , Dore, E. and Morgeneyer, M. . (2013) Investigation of the Release of Particles from a Nanocoated Product. Advances in Nanoparticles; 39-44.

Lin W, Huang Y-w, Zhou X-D, Ma Y. (2006) In vitro toxicity of silica nanoparticles in human lung cancer cells. Toxicology and Applied Pharmacology; 217 252-59.

Mazzuckelli LF, Methner MM, Birch ME, Evans DE, Ku B-K, Crouch K, Hoover MD. (2007) Identification and Characterization of Potential Sources of Worker Exposure to Carbon Nanofibers During Polymer Composite Laboratory Operations. Journal of Occupational and Environmental Hygiene; 4 D125-D30.

Methner M, Crawford C, Geraci C. (2012) Evaluation of the potential airborne release of carbon nanofibers during the preparation, grinding, and cutting of epoxy-based nanocomposite material. J Occup Environ Hyg; 9 308-18.

Ogura I, Kotake M, Shigeta M, Uejima M, Saito K, Hashimoto N, Kishimoto A. (2013) Potential release of carbon nanotubes from their composites during grinding. Journal of Physics: Conference Series; 429 012049.

Patel MM, Miller MA, Chomchai S. (2006) Polymer fume fever after use of a household product. The American Journal of Emergency Medicine; 24 880-81.

Poland CA, Duffin R, Kinloch I, Maynard A, Wallace WAH, Seaton A, Stone V, Brown S, MacNee W, Donaldson K. (2008) Carbon nanotubes introduced into the abdominal cavity of mice show asbestos-like pathogenicity in a pilot study. Nat Nano; 3 423-28.

R. Satheesh Raja KM, V. Manikandan Effect of Carbon Black and Fly Ash Fillers on Tensile Properties of Composites Key Engineering Materials; 471-472 26-30

Rudolph D D, Kalidas R P. (1976) Carbon Black Embrittlement of ABS. Toughness and Brittleness of Plastics: AMERICAN CHEMICAL SOCIETY.

Saber AT, Jacobsen NR, Mortensen A, Szarek J, Jackson P, Madsen AM, Jensen KA, Koponen IK, Brunborg G, Gutzkow KB*, et al.* (2012) Nanotitanium dioxide toxicity in mouse lung is reduced in sanding dust from paint. Part Fibre Toxicol; 9 4.

Saber AT, Koponen IK, Jensen KA, Jacobsen NR, Mikkelsen L, Moller P, Loft S, Vogel U, Wallin H. (2012) Inflammatory and genotoxic effects of sanding dust generated from nanoparticle-containing paints and lacquers. Nanotoxicology; 6 776-88.

Saber AT, Mortensen A, Szarek J, Koponen IK, Levin M, Jacobsen NR, Pozzebon ME, Mucelli SP, Rickerby DG, Kling K*, et al.* (2016) Epoxy composite dusts with and without carbon nanotubes cause similar pulmonary responses, but differences in liver histology in mice following pulmonary deposition. Particle and Fibre Toxicology; 13 37.

Sachse S, Silva F, Irfan A, Zhu H, Pielichowski K, Leszczynska A, Blazquez M, Kazmina O, Kuzmenko O, Njuguna J. (2012) Physical characteristics of nanoparticles emitted during drilling of silica based polyamide 6 nanocomposites. IOP Conference Series: Materials Science and Engineering; 40 012012.

Sachse S, Silva F, Zhu H, Irfan A, Leszczy A, Pielichowski K, Ermini V, Blazquez M, Kuzmenko O, Njuguna J. (2012) The effect of nanoclay on dust generation during drilling of PA6 nanocomposites. J. Nanomaterials; 2012 26-26.

Schlagenhauf L, Buerki-Thurnherr T, Kuo Y-Y, Wichser A, Nüesch F, Wick P, Wang J. (2015) Carbon Nanotubes Released from an Epoxy-Based Nanocomposite: Quantification and Particle Toxicity. Environmental Science & Technology; 49 10616-23.

Schlagenhauf L, Chu BTT, Buha J, Nüesch F, Wang J. (2012) Release of Carbon Nanotubes from an Epoxy-Based Nanocomposite during an Abrasion Process. Environmental Science & Technology; 46 7366-72.

Schlagenhauf L, Nüesch F, Wang J. (2014) Release of Carbon Nanotubes from Polymer Nanocomposites. Fibers; 2 108.

Shandilya N, Le Bihan O, Morgeneyer M. (2014) Effect of the Normal Load on the Release of Aerosol Wear Particles During Abrasion. Tribology Letters; 55 227-34.

Sotiriou GA, Singh D, Zhang F, Chalbot M-CG, Spielman-Sun E, Hoering L, Kavouras IG, Lowry GV, Wohlleben W, Demokritou P. (2016) Thermal decomposition of nano-enabled thermoplastics: Possible environmental health and safety implications. Journal of Hazardous Materials; 305 87-95.

Sotiriou GA, Singh D, Zhang F, Wohlleben W, Chalbot M-CG, Kavouras IG, Demokritou P. (2015) An integrated methodology for the assessment of environmental health implications during thermal decomposition of nano-enabled products. Environmental Science: Nano; 2 262-72.

Szeluga U, Kumanek B, Trzebicka B. (2015) Synergy in hybrid polymer/nanocarbon composites. A review. Composites Part A: Applied Science and Manufacturing; 73 204-31.

Testud F, Sabouraud S, Lecoq-Jammes F. (2010) Fièvre des polymères après fartage intensif de snowboards en milieu confiné : 3 observations. Archives des Maladies Professionnelles et de l'Environnement; 71 925-30.

Townsend PW, Vernice GG, Williams RL. (1989) 'Polymer fume fever' without polymer. Journal of Fluorine Chemistry; 42 441-43.

Tsai S, Ashter A, Ada E, Mead J, Barry C, Ellenbecker M. (2008) Control of Airborne Nanoparticles Release During Compounding of Polymer Nanocomposites. Nano; 3 301 - 09.

Van Krevelen DW, Te Nijenhuis K. (2009) Chapter 13 - Mechanical Properties of Solid Polymers. In by, DWVK, Nijenhuis, KT editors. Properties of Polymers (Fourth Edition), Amsterdam: Elsevier.

Van Landuyt KL, Yoshihara K, Geebelen B, Peumans M, Godderis L, Hoet P, Van Meerbeek B. (2012) Should we be concerned about composite (nano-)dust? Dental Materials; 28 1162-70.

Wohlleben W, Brill S, Meier M, Mertler M, Cox G, Hirth S, von Vacano B, Strauss V, Treumann S, Wiench K*, et al.* (2011) On the Lifecycle of nanocomposites: Comparing Released Fragments and their In-Vivo Hazards from Three Release Mechanisms and Four Nanocomposites. Small.

Wohlleben W, Meier MW, Vogel S, Landsiedel R, Cox G, Hirth S, Tomovic Z. (2013) Elastic CNT-polyurethane nanocomposite: synthesis, performance and assessment of fragments released during use. Nanoscale; 5 369-80.

Wohlleben W, Meyer J, Muller J, Muller P, Vilsmeier K, Stahlmecke B, Kuhlbusch TAJ. (2016) Release from nanomaterials during their use phase: combined mechanical and chemical stresses applied to simple and multi-filler nanocomposites mimicking wear of nano-reinforced tires. Environmental Science: Nano; 3 1036-51.

Zhang H, Kuo Y-Y, Gerecke AC, Wang J. (2012) Co-Release of Hexabromocyclododecane (HBCD) and Nano- and Microparticles from Thermal Cutting of Polystyrene Foams. Environmental Science & Technology; 46 10990-96.

Table 2. Drilling test parameters.

		Drilling speed, rpm		
		1200 (S3)	1550 (S5)	1880 (S7)
Drill bit size, mm	4	-	All	SiO_2
	8	MWCNT	MWCNT	All

*Entire range of drilling speeds: 900–2,900 rpm from settings (S) 1-10.

Replicate Test	PU		PU/CNT		PU/SiO_2		PU/CB	
	N, #/cm^3	D, nm	N, #/cm^3	D, nm	N, #/cm^3	D, nm	N, #/cm^3	D, nm
Background	262	-	288	-	186	-	141	-
Drill 1	743	63.7	626	101.5	649	85.3	581	59.7
Drill 2	648	54.1	540	97.7	732	65.6	610	53.1
Drill 3	651	51.1	577	89.7	651	60.9	573	53.8
Drill 4	640	71.0	501	94.7	656	60.8	558	55.1
Drill 5	695	52.0	585	100.5	-	-	693	58.8
Mean	675	58.4	566	96.8	680	68.1	603	56.1
S.D.	38.8	7.7	42.2	4.3	37.4	10.1	48.0	2.7
S.D., %	5.74%	13.27%	7.46%	4.42%	5.50%	14.78%	7.95%	4.78%

Table 2. Particle number concentration, N (#/cm^3), and geometric mean diameter, D (nm), for replicate tests (Φ/drill, 4 mm; drill speed setting, S5). All measurements recorded with a DISCmini (size range 10–300 nm). The differences in particle number were statistically significant for PU-PU/CNT pair (P=0.0052) and for PU-PU/CB pair (P=0.0473), but not for PU-PU/SiO_2 pair (P=0.9075). The difference in size was only significant for PU-PU/CNT pair (P=0.0001), but not for PU-PU/SiO_2 pair (P=0.1905) and PU-PU/CB pair (P=0.6103).

	OPC (250 nm – 32 μm), #/cm^3				DISCmini (10–300 nm), #/cm^3			
	PU	PU/CNT	PU/SiO_2	PU/CB	PU	PU/CNT	PU/SiO_2	PU/CB
Backgr.	0.001	0.001	0.021	0.020	40	36	89	30
Cut 1	0.404	1.714	0.519	6.025	36	66	63	57
Cut 2	0.284	1.349	0.489	5.580	30	63	66	46
Cut 3	0.409	1.069	0.594	5.290	1	50	118	44
Cut 4	0.259	1.279	0.384	4.715	-12	50	66	42
Cut 5	0.319	1.074	-	-	14	101	-	-
Mean	**0.335**	**1.297**	**0.497**	**5.403**	**13.75**	**57.25**	**78.25**	**47.25**
S.D.	0.069	0.264	0.087	0.549	19.9	20.9	26.5	6.7
S.D., %	20.6%	20.4%	17.5%	10.2%	144%	36.5%	33.9%	14.2%

Table 3. Summary of particle number concentration results for different samples during the sawing process (results for cut 1 to 5 are background corrected. Note: The default unit of the OPC readings is #/L and it is converted into #/cm^3 in the table for comparison purposes). The difference in OPC mean particle concentrations for the four sample types was significant ($p<0.001$); pairwise differences were all significant ($p<0.05$). DISCmini measurements were below the detection limit of 1000 #/cm^3 established by the manufacturer. The difference in DISCmini machine readouts of the mean particle concentrations for the four sample types was significant ($p=0.0013$); pairwise differences were all significant: PU-PU/MWCNT ($p=0.004$), PU-PU/SiO2 ($p=0.004$) and PU-PU/CB ($p=0.015$).

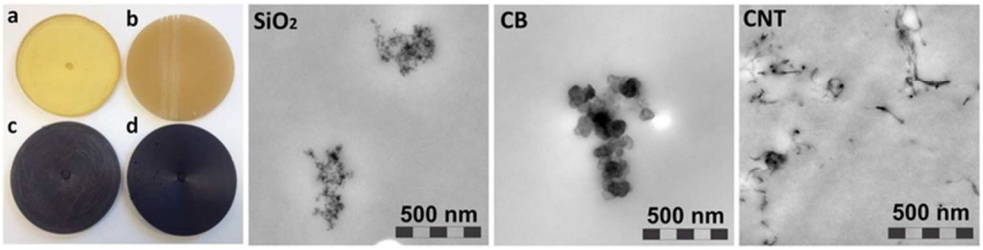

Figure 1. Photo of tested samples (a - PU; b - PU/SiO2; c - PU/CB; d - PU/MWCNT) and TEM images of a cross-section of the samples with the three filler types. Sample dimensions: 11 cm Φ x 1.0 cm thickness, disc.

66x17mm (300 x 300 DPI)

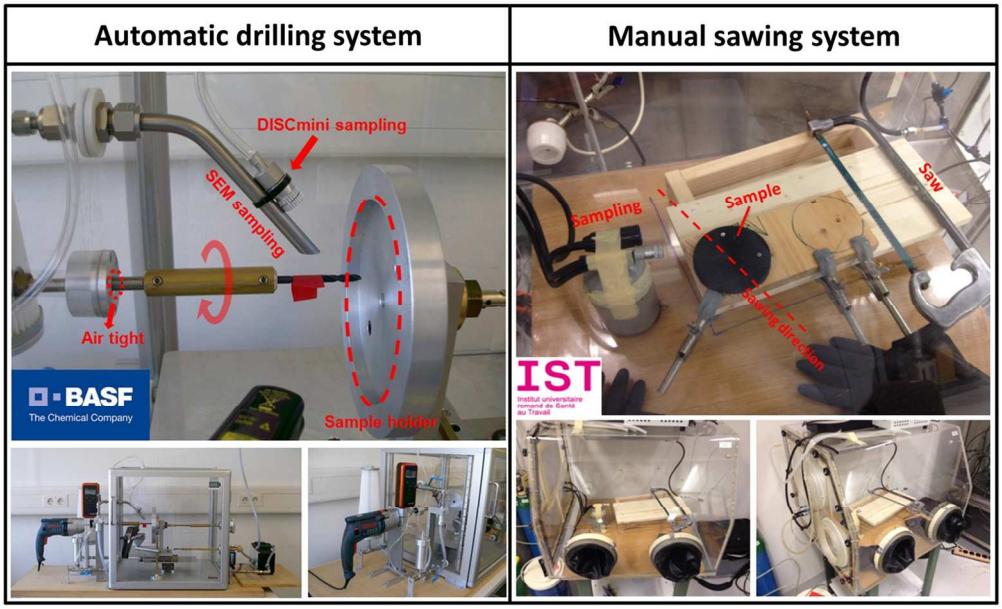

Figure 2 Photos of the drilling (left) and sawing (right) setups used in the tests

137x83mm (300 x 300 DPI)

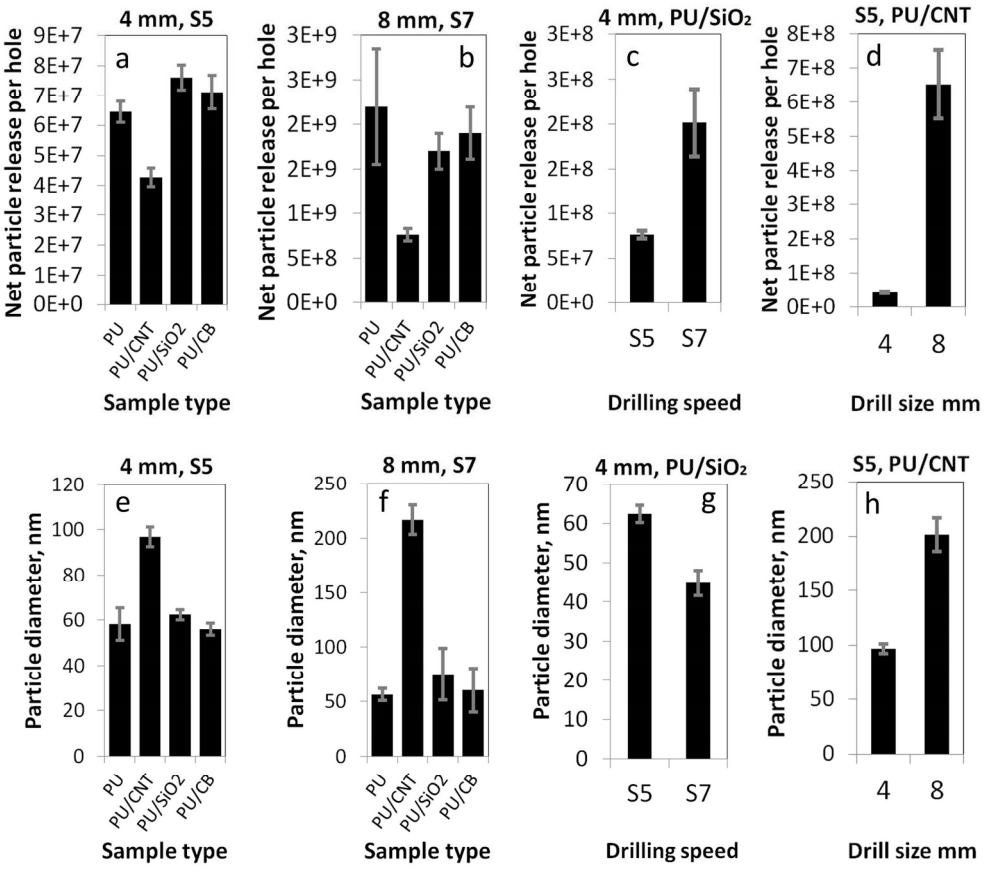

Figure 3. Influence of types of nanomaterial filler, drill speed setting (S5 or S7), and bit diameter (4 mm or 8 mm) on the net release of particles and their mean diameter (size range: 10–300 nm). The statistical analysis: a) p=0.0056 (group), p=0.013 (PU-PU/CNT pair), p>0.1 (other pairs); b) p=0.004 (group), p=0.0205 (PU-PU/CNT pair), p>0.1 (other pairs); c) p=0.006; d) p<0.001; d) p=0.006; d) p<0.001;e) p<0.001 (group), p<0.001 (PU-PU/CNT pair), p>0.1 (other pairs); f) p<0.001 (group), p<0.001 (PU-PU/CNT pair), p>0.1 (other pairs). g) p<0.001; h) p<0.001.

190x165mm (300 x 300 DPI)

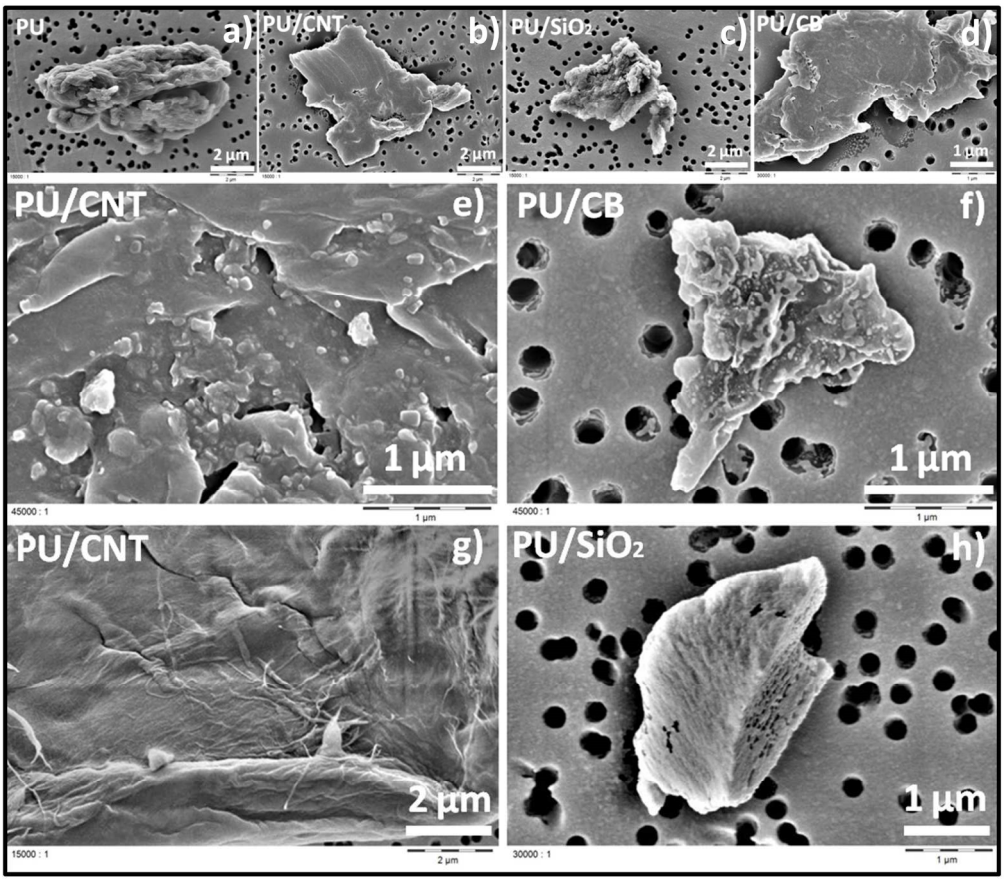

Figure 4. Surface morphologies of particles released in the drilling tests.

188x165mm (300 x 300 DPI)

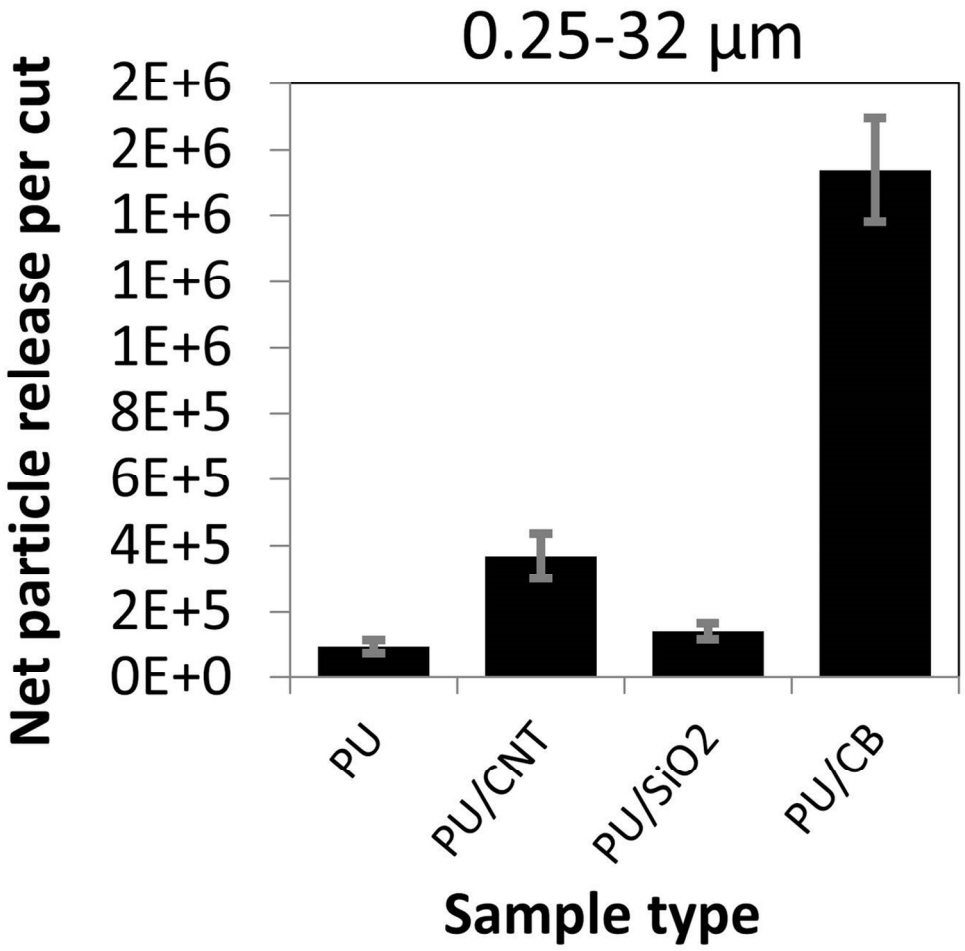

Figure 5. Influence of type of filler on particle release (net release after background correction) in the size range 0.25–32 µm (data from OPC).

112x110mm (300 x 300 DPI)

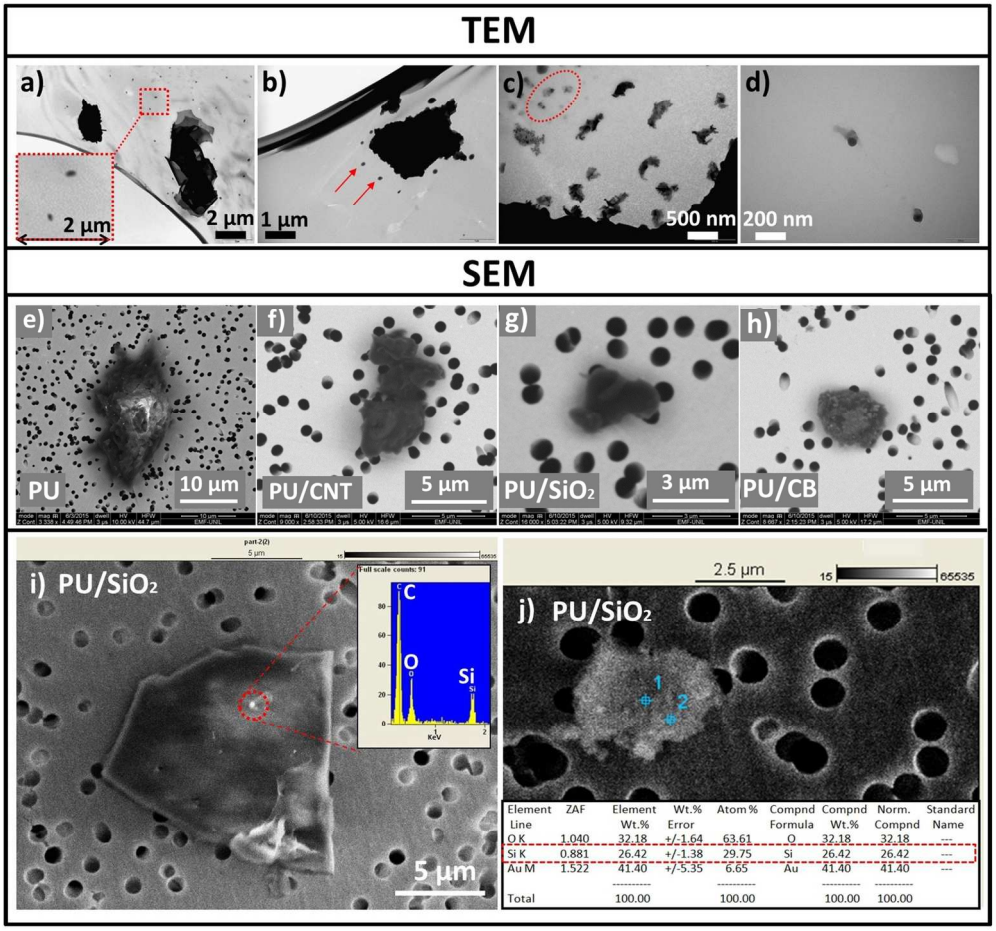

Figure 6. TEM and SEM observations of released particles from the sawing tests: a–d, PU.

188x176mm (300 x 300 DPI)